IMPLEMENTATION OF THE STABILIZED THREE-FIELD FORMULATION

FRANCO BREZZI[†§], L. DONATELLA MARINI[†§]

Abstract. This paper deals with the computational aspects of the so-called three-field formulation, introduced first in [6] and analysed in [8]. In particular, we introduce the possible use of *virtual bubbles* (in the basic framework of [1]) and we show that their use can simplify the implementation of the method. A variety of numerical experiments is also presented. They show that the use of virtual bubbles instead of conventional ones does not affect the quality of the final accuracy. More generally, they show clearly the general robustness of the three-field formulation, together with the possibility of using powerful preconditioners when the interface grid is chosen to be uniform.

1. Introduction. Let us briefly recall, for the convenience of the reader, the main idea of the three-field formulation. Assume that we have to solve a linear elliptic problem whose variational formulation is given by:

$$\text{find } w \in V \text{ such that} \qquad a(w,v) = (f,v) \qquad \forall v \in V, \tag{1.1}$$

on a domain Ω. We assume that the problem is associated to a second-order differential operator, so that the space V will be a subspace of $H^1(\Omega)$. By splitting Ω into subdomains Ω^s one introduces suitable subspaces V^s of $H^1(\Omega^s)$, and defines $M^s = H^{-1/2}(\partial\Omega^s)$, $\Sigma = \cup_s \partial\Omega^s$, and $\Phi = \{\text{traces on } \Sigma \text{ of the functions of } V\}$. Setting $V^* := \mathbf{\Pi}_s V^s$ and $M^* := \mathbf{\Pi}_s M^s$, the three-field formulation of (1.1) then reads

$$\left\{\begin{array}{lllll} \text{find } u \in V^*,\ \lambda \in M^*, & \text{and } \psi \in \Phi \text{ such that} & & & \\ \text{i)} \quad a_s(u^s,v) - <\lambda^s, v>_s & = (f,v)_s & \forall v \in V^s & \forall s & \\ \text{ii)} \quad <\mu^s, u_s>_s & = <\mu^s, \psi>_s & \forall \mu^s \in M^s & \forall s & \\ \text{iii)} \ \sum_s <\lambda^s, \varphi>_s & = 0 & \forall \varphi \in \Phi & & \end{array}\right. \tag{1.2}$$

with obvious meaning for a_s, $<.,.>_s$ and $(.,.)_s$ (see also (2.2)- (2.3) in the next section). This formulation was originally introduced in [6], [7], where it was proved that, under reasonable assumptions, problem (1.2) has a unique solution related to the solution of (1.1) by

$$\left\{\begin{array}{lll} \text{i)} \quad u^s & = w_{|\Omega^s} & \text{for each } s \\ \text{ii)} \quad \lambda^s & = \dfrac{\partial w}{\partial n_a}_{|\partial\Omega^s} & \text{for each } s \\ \text{iii)} \ \psi & = w_{|\Sigma}, & \end{array}\right. \tag{1.3}$$

with $\frac{\partial}{\partial n_a}_{|\partial\Omega^s}$ = outward conormal derivative to $\partial\Omega^s$. For other interesting variants of (1.2) see [14]. In order to approximate (1.2) one has to choose, for every s, finite dimensional subspaces V_h^s, M_h^s and Φ_h of V^s, M^s and Φ respectively, to construct $V_h^* := \mathbf{\Pi}_s V_h^s$ and $M_h^* := \mathbf{\Pi}_s M_h^s$, and to consider the following discretized problem:

$$\left\{\begin{array}{lllll} \text{find } u_h \in V_h^*,\ \lambda_h \in M_h^*, & \text{and } \psi_h \in \Phi_h \text{ such that} & & & \\ \text{i)} \quad a_s(u_h^s,v) - <\lambda_h^s, v>_s & = (f,v)_s & \forall v \in V_h^s & \forall s & \\ \text{ii)} \quad <\mu^s, u_h^s>_s & = <\mu^s, \psi_h>_s & \forall \mu^s \in M_h^s & \forall s & \\ \text{iii)} \ \sum_s <\lambda_h^s, \varphi>_s & = 0 & \forall \varphi \in \Phi. & & \end{array}\right. \tag{1.4}$$

*Dipartimento di Matematica, Università di Pavia, via Ferrata 1, 27100 Pavia, Italy
†Istituto di Analisi Numerica del CNR, via Ferrata 1, 27100 Pavia, Italy

If the three families of subspaces are suitably chosen, problem (1.4) will be well posed, and its solution will converge to the exact solution of (1.2) with optimal order. In general, the finite element spaces Φ_h, V_h^s and M_h^s will be based on three corresponding decompositions, that cannot be chosen arbitrarily. In [8], we considered the case where two independent choices are given, a priori, for Φ_h and V_h^s. It seems particularly reasonable to assume the grid for Φ_h as given, since in many cases this will be the space were multidomain preconditioners (for the Schur complement) will be applied: to have a convenient grid might then allow the use of more powerful preconditioners (see for instance [11], [13], [2], [4], [17], [12], [15], [16].) Similarly, it is also reasonable to assume the grid for V_h^s as given, as it is often the case for real applications, where the nature of the original problem (1.1) dictates different grids in different parts of the domain. Let us assume, for simplicity, that both Φ_h and V_h^s are made of piecewise linear continuous functions. The task is then to start from the two given grids, and to reach, with minor modifications, a problem of the type (1.4) which is well posed and optimally convergent. The main idea of [5], made precise and perfectioned in [9] and then in [8], was to chose first a suitable grid for the multipliers M_h^s, in each subdomain, starting from the given grids $\mathscr{T}_\psi$ (for ψ at the interfaces) and $\mathscr{T}_u^s$ (for u within each subdomain). Essentially, the choice considered was to take, in each subdomain,

$$\mathscr{T}_\lambda^s = \text{ merge } \{(\mathscr{T}_u^s)_{|\Gamma^s}, (\mathscr{T}_\psi)_{|\Gamma^s}\} \qquad \forall s. \tag{1.5}$$

Once the grids $\mathscr{T}_\lambda^s$ were given, the spaces M_h^s were chosen as piecewise constants on $\mathscr{T}_\lambda^s$. In general, this choice cannot actually guarantee stability. However, the idea was to increase artificially the original spaces V_h^s with the addition of *boundary bubbles* (essentially: functions having support in a single boundary triangle.) If, for every s, B_h^s is the space of bubbles to be used in order to augment the space V_h^s, we replace then V_h^s by the augmented space

$$\widetilde{V}_h^s \ = \ V_h^s \oplus B_h^s \qquad \forall s. \tag{1.6}$$

Setting finally $\widetilde{V}_h^* = \mathbf{\Pi}_s \widetilde{V}_h^s$, the stabilized discrete problem becomes

$$\left\{ \begin{array}{lllll} \text{find } u_h \in \widetilde{V}_h^*, \ \lambda_h \in M_h^* \text{ and } \psi_h \in \Phi_h & \text{such that} & & & \\ \text{i)} \quad a_s(u_h^s, v) - <\lambda_h^s, v>_s & = \ (f, v)_s & \forall v \in \widetilde{V}_h^s & \forall s \\ \text{ii)} \quad <\mu^s, u_h^s>_s & = \ <\mu^s, \psi_h>_s & \forall \mu^s \in M_h^s & \forall s \\ \text{iii)} \ \sum_s <\lambda_h^s, \varphi>_s & = 0 & \forall \varphi \in \Phi_h. & \end{array} \right. \tag{1.7}$$

All this will become clearer, and more precise, in the next sections, where a particular case will be considered. For the time being, we just point out that, under reasonable assumptions on the original given grids $\mathscr{T}_\psi$ and $\mathscr{T}_u^s$, we were able to indicate a suitable choice of piecewise quadratic boundary bubbles, whose addition makes (1.7) stable and optimally convergent. Moreover, (see also [9]), it is possible to eliminate a priori *both* the bubbles and the multipliers in such a way that, in each subdomain, one is left with a problem in the only (original) unknown u_h.

In the present paper, we reconsider the choice of the bubble functions, that we now allow to be much more general. In particular, we show that the elimination process can be simplified with a nonstandard choice of the bubble shape. We also indicate explicitly a possible very effective preconditioner that can be used if the grid $\mathscr{T}_\psi$ is uniform, and we test it on a model problem. More generally, we performed several

series of tests, always on a simple model problem, in order to assess the robustness of the method.

An outline of the paper is as follows. In section 2, we choose the model problem, and we present, in this particular case, the spaces to be used, the type of bubbles that we are going to use, and the corresponding elimination procedure in more detail. Always on the model problem, we describe the preconditioner as well. In section 3 we present the numerical results that we have obtained. The possible parameters that we might have taken into account are several: the ratio between the two abutting grids for u, the ratio among the grids for u and for ψ, the shape of the bubbles, and the general behaviour when all the meshes are refined (say, halved) at the same time. We tried to point out the most meaningful among those relationships. In particular, the theoretical error bounds proved in [8] are fully verified, even with the present more general bubble shape.

2. The problem, the spaces and the bubbles. In order to simplify the presentation, we confine ourselves on a particularly simple toy-problem. It should be clear, however, that all the contents of this section can be very easily extended to much more complex situations.

We assume therefore that our bilinear form $a(u,v)$ is associated with the Laplace operator:

$$a(u,v) = \int_\Omega \nabla u \cdot \nabla v \mathrm{d}x\, \mathrm{d}y. \tag{2.1}$$

Always to make life simple, assume that Ω is the rectangle $]-1,1[\times]0,1[$, split into $\Omega^1 =]-1,0[\times]0,1[$ and $\Omega^2 =]0,1[\times]0,1[$. Accordingly, we set

$$a_s(u,v) = \int_{\Omega_s} \nabla u \cdot \nabla v \, \mathrm{d}x\, \mathrm{d}y, \tag{2.2}$$

for $s = 1,2$. Similarly we set

$$< u, v >_s = \int_{\partial\Omega^s} u\, v \, d\Gamma \qquad (u,v)_s = \int_{\Omega^s} u\, v \, \mathrm{d}x\, \mathrm{d}y \tag{2.3}$$

For the time being, we consider homogeneous Dirichlet boundary conditions on $\partial\Omega$, although the numerical experiments have been done with nonhomogeneous ones. It is true that, in the finite element context, nonhomogeneous Dirichlet boundary conditions are easier to implement than to explain. Accordingly, we then have

$$V = H_0^1(\Omega), \qquad V^s = \{v \in H^1(\Omega^s), \quad v = 0 \quad on \quad \partial\Omega\}, \quad s = 1,2. \tag{2.4}$$

We assume that we are given a (uniform) decomposition $\mathscr{T}_\psi$ of the interface, and two given decompositions $\mathscr{T}_u^1$ and $\mathscr{T}_u^2$ of Ω^1 and Ω^2 respectively. For simplicity, we might also assume that they are both uniform (right triangles), as those used in the numerical experiments, although this is not really necessary. What is important, in order to have a meaningful case, is that the two decompositions *do not* agree on the interface $\Sigma = \{0\}\times]0,1[$. We consider then, as we announced in the introduction, the spaces Φ_h, V_h^1 and V_h^2 as made of piecewise linear continuous functions on the given decompositions. We then use the basic idea (1.5) to define the grids for the multiplier, which are given here by

$$\mathscr{T}_\lambda^s = \text{ merge } \{(\mathscr{T}_u^s)_{|\Sigma}, (\mathscr{T}_\psi)\} \qquad s = 1,2, \tag{2.5}$$

and we take M_h^1 and M_h^2 made of piecewise constants on their respective grids. Then $M_h^* = M_h^1 \times M_h^2$.

We are now ready for the introduction of the bubbles. We restrict our attention to Ω^1. The procedure on Ω^2 will be identical. Let T be a triangle in $\mathcal{T}_u^1$ having an edge L on Σ, and let P be the vertex of T opposite to L. Let now $I_1, ...I_K$ be the intervals of $\mathcal{T}_\lambda^1$ contained in L. For every $k = 1, .., K$ we consider the triangle T_k having I_k as one edge, and P as opposite vertex. Applying this procedure to every triangle having an edge on Σ, we obtain as many subtriangles T_k as there are intervals in $\mathcal{T}_\lambda^1$. For every subtriangle T_k we choose now *one* function b_k, with the following properties: we assume that $\int_{I_k} b_k$ is different from zero, so that we can normalise it to one. We also assume that b_k vanishes identically on the other two edges of T_k. When convenient, we shall identify b_k with its extension by zero on Ω^1, that will clearly belong to V^1. We now call B^1 the subspace of V^1 spanned by all the *bubbles* b_k, and we set, as in (1.6)

$$\widetilde{V}^1 = V^1 \oplus B^1. \tag{2.6}$$

By applying the same procedure in Ω^2 we will obtain a space $\widetilde{V}^2$ that, together with $\widetilde{V}^1$, gives then rise to $\widetilde{V}_h^* = \widetilde{V}^1 \times \widetilde{V}^2$. With all the spaces made precise we can now reconsider the stabilized problem (1.7), that we report here for the convenience of the reader:

$$\left\{\begin{array}{llll} \text{find } u_h \in \widetilde{V}_h^*,\ \lambda_h \in M_h^* \text{ and } \psi_h \in \Phi_h & \text{such that} & & \\ \text{i)} \quad a_s(u_h^s, v) - <\lambda_h^s, v>_s & = \ (f, v)_s & \forall v \in \widetilde{V}_h^s & s = 1, 2 \\ \text{ii)} \quad <\mu^s, u_h^s>_s & = \ <\mu^s, \psi_h>_s & \forall \mu^s \in M_h^s & s = 1, 2 \\ \text{iii)} \ \sum_s <\lambda_h^s, \varphi>_s & = 0 & \forall \varphi \in \Phi_h. & \end{array}\right. \tag{2.7}$$

Looking at (2.7) it is clear that, for fixed ψ_h, the first two equations can be solved independently and *in parallel*. We can therefore consider the mapping $\mathscr{S}_h = (\mathscr{S}_u, \mathscr{S}_\lambda)$ that associates to the pair (f, ψ_h) the solution (u_h, λ_h) of the first two equations of (2.7). With this notation, problem (2.7) can be written as:

$$\text{find } \psi_h \in \Phi_h \text{ such that} \qquad \sum_{s=1}^{2} <\mathscr{S}_\lambda(f, \psi_h), \varphi>_s = 0, \qquad \forall \varphi \in \Phi_h. \tag{2.8}$$

It is clear that in (2.8) a crucial role is played by the linear operator S_h, from Φ_h to its dual space, defined by:

$$<S_h(\psi_h), \varphi> := \sum_{s=1}^{2} <\mathscr{S}_\lambda(0, \psi_h), \varphi>_s, \tag{2.9}$$

which is commonly called Schur complement, and whose spectral properties have a paramount relevance in solving (2.8) by iterative methods. We shall come back to this very important point when discussing the preconditioner.

For the time being, we concentrate first on the procedure of eliminating bubbles and multipliers. As we shall see, the procedure can be implemented, separately and in parallel, in each subdomain Ω^s. Hence, to describe it, we concentrate on a single domain. We assume ψ_h to be given, and we see how to compute the corresponding u_h^s and λ_h^s. For the sake of simplicity, we might drop at this point the superscript s, as the same identical procedure will be applied, in parallel, in each subdomain. With an

abuse of notation, we are also going to call Ω (instead of Ω^s) the current subdomain, and so on. No confusion should arise. With this simplified notation the local problem becomes:

$$\begin{cases} \text{given } \psi_h \text{ on } \partial\Omega, \text{ find } u_h \in \widetilde{V}_h & \text{and } \lambda_h \in M_h & \text{such that} \\ \text{i)} \quad a(u_h, v) - <\lambda_h, v> & = (f, v) & \forall v \in \widetilde{V}_h \\ \text{ii)} \quad <\mu, u_h> & = <\mu, \psi_h> & \forall \mu \in M_h, \end{cases} \tag{2.10}$$

where M_h is made of piecewise constants on $\mathscr{T}_\lambda$, and $\widetilde{V}_h$ is obtained as the sum of piecewise linear functions on $\mathscr{T}_u$ (that we will denote by V_L,) and the space of boundary bubbles B_h. Accordingly, u_h will be written as

$$u_h(x) = u_L(x) + \sum_k u_B^k \, b_k(x), \tag{2.11}$$

where k ranges now on the set of all the bubbles.

From the second equation of (2.10), by taking μ as the characteristic function of an interval I_k of $\mathscr{T}_\lambda$, we obtain:

$$u_B^k = \left(\int_{I_k} \psi_h \mathrm{d}\Gamma - \int_{I_k} u_L \mathrm{d}\Gamma \right) / \int_{I_k} b_k \mathrm{d}\Gamma. \tag{2.12}$$

We remark that both u_L and ψ_h are linear in each I_k. We also remind that the bubbles were normalized in such a way that $\int_{I_k} b_k \mathrm{d}\Gamma = 1$ for all k. Therefore, indicating by m_k the midpoint of I_k, we immediately obtain from (2.12) that

$$u_B^k = (\psi_h(m_k) - u_L(m_k))|I_k|. \tag{2.13}$$

We can now use the first equation of (2.10), with $v = b_k$, in order to express λ_k as a function of the other variables:

$$\lambda_k = a(u_L, b_k) + u_B^k \, a(b_k, b_k) - (f, b_k). \tag{2.14}$$

Assume now, for simplicity, that the right-hand side f is piecewise constant. This is not really restrictive, as in most cases f is approximated anyhow by a piecewise constant in the actual implementation. We remark now that, integrating by parts, for every $v_L \in V_L$ and for every k we have:

$$a(v_L, b_k) = a(b_k, v_L) = \int_{I_k} \frac{\partial v_L}{\partial n} b_k \mathrm{d}\Gamma = \frac{\partial v_L}{\partial n}, \tag{2.15}$$

where clearly $\partial v_L / \partial n$ is the (constant) outward normal derivative of v_L in the triangle (of $\mathcal{T}_u$) containing T_k. We also set:

$$\gamma_k^T = \int_{T_k} b_k \mathrm{d}x \, \mathrm{d}y, \qquad \gamma_k^a = a(b_k, b_k), \tag{2.16}$$

so that (2.14) becomes

$$\lambda_k = \frac{\partial u_L}{\partial n} + u_B^k \gamma_k^a - f_k \gamma_k^T. \tag{2.17}$$

With some manipulations, using (2.13) and (2.15), we obtain

$$a(\sum_k u_B^k \, b_k, v_L) = \int_{\partial\Omega} (\psi_h - u_L) \frac{\partial v_L}{\partial n} \mathrm{d}\Gamma. \tag{2.18}$$

Taking now the first equation of (2.10) for $v = v_L$, using (2.13) (2.17) and (2.15), we obtain with easy computations that

$$a(u_L, v_L) - < u_L, \frac{\partial v_L}{\partial n} > - < v_L, \frac{\partial u_L}{\partial n} > + \sum_k |I_k|^2 \gamma_k^a \, u_L(m_k) v_L(m_k) =$$
$$(f, v_L) - \sum_k f_k \gamma_k^T |I_k| v_L(m_k) - < \psi_h, \frac{\partial v_L}{\partial n} > + \sum_k |I_k|^2 \gamma_k^a \, \psi_h(m_k) v_L(m_k). \tag{2.19}$$

At this point we have to discuss the actual shape of the bubble functions. Neglecting for a while the problem related to the coefficient γ_k^T in (2.16) we remark that, having fixed the integral of b_k on I_k to be one, the coefficient γ_k^a has a *lower bound* which depends on the shape of T_k. In particular we have the following result.

Theorem *Let T be a triangle, and ℓ one of its edges. Let v be an element of $H^1(T)$ vanishing on the other two edges of T. Assume that $\int_\ell v \, d\Gamma = 1$. Then $|v|_{1,T} \geq |w|_{1,T}$, where w is the unique harmonic function on T such that $\partial w/\partial n =$ constant on ℓ and $w = 0$ at the other two edges of T, scaled in such a way that $\int_\ell w \, d\Gamma = 1$.*

Proof. The result comes out easily by minimising the quantity $|v|^2_{1,T}$ under the constraint $\int_\ell v \, d\Gamma = 1$. Let w be the minimizer. Then, by the usual technique of Lagrange multipliers, we have that

$$\int_T \nabla w \cdot \nabla \zeta \mathrm{d}x \, \mathrm{d}y = c \int_\ell \zeta \mathrm{d}\Gamma. \tag{2.20}$$

for all $\zeta \in H^1(T)$ vanishing on $\partial T \setminus \ell$, where c is a suitable constant to be determined. The result follows immediately. ∎

We consider first a fixed triangle, say $\hat{T}$, having vertices in $(0,0)$, $(1,1)$, and $(1,-1)$. Here a harmonic function $\hat{w}$ having constant normal derivative on the edge $\hat{\ell}$ of equation $x = 1$ and vanishing on the other two edges is easily found: actually we have $\hat{w} = x^2 - y^2$. For this function we have

$$|\hat{w}|^2_{1,\hat{T}} = 8/3, \qquad \int_{\hat{\ell}} \hat{w} \mathrm{d}\Gamma = 4/3, \qquad \int_{\hat{T}} \hat{w} \mathrm{d}x\mathrm{d}y = 1/3. \tag{2.21}$$

For any positive t we can now scale the triangle $\hat{T}$ down to a new triangle T_t having vertices in (0,0), (t,t), and $(t,-t)$. If w_t is the image of $\hat{w}$ in T_t (that means that $w_t = (x/t)^2 - (y/t)^2$), we easily get

$$|w_t|^2_{1,T_t} = 8/3, \qquad \int_{\ell_t} w_t \mathrm{d}\Gamma = 4t/3, \qquad \int_{T_t} w_t \mathrm{d}x\mathrm{d}y = t^2/3. \tag{2.22}$$

Assume, for simplicity, that the two angles of T_k insisting on the edge I_k are both $\geq \pi/4$, as it was the case in our tests. Hence, we can always insert a triangle like T_t inside T_k, (see figure 2.1.) Notice that in this case we shall have $t = |I_k|/2$. In order to normalize the boundary integral to one, we set then

$$b_k = \frac{3}{4t} w_t \qquad in \quad T_t, \tag{2.23}$$

and $b_k = 0$ in the rest of T_k. Recalling (2.22) and $t = |I_k|/2$, we have therefore

$$\gamma_k^a = |b_k|^2_{1,T_k} = 6|I_k|^{-2}, \qquad \int_{I_k} b_k \mathrm{d}\Gamma = 1, \qquad \gamma_k^T = \int_{T_k} b_k \mathrm{d}x\mathrm{d}y = |I_k|/8. \tag{2.24}$$

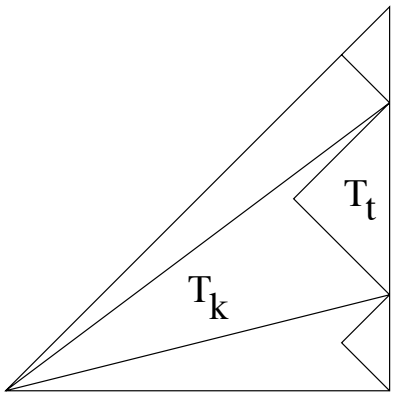

FIG. 2.1.

We see therefore, in particular, that the lower bound for γ_k^a will always be $\leq 6|I_k|^{-2}$. Substituting (2.24) in (2.19) yields:

$$\begin{aligned} &a(u_L, v_L) - < u_L, \frac{\partial v_L}{\partial n} > - < v_L, \frac{\partial u_L}{\partial n} > + \textstyle\sum_k 6\, u_L(m_k) v_L(m_k) = \\ &(f, v_L) - \textstyle\sum_k f_k \frac{1}{8} |I_k|^2 v_L(m_k) - < \psi_h, \frac{\partial v_L}{\partial n} > + \textstyle\sum_k 6\, \psi_h(m_k) v_L(m_k), \end{aligned} \tag{2.25}$$

whose implementation is reasonably easy.

We can also consider other possible choices of the bubble shape. In particular we could think of choosing a bubble function b_k such that its integral over T_k vanishes. This would make the second term in the right-hand side of (2.19) equal to zero. One possibility is to consider a new bubble still given by (2.23) in T_t, but which is now different from zero somewhere else in T_k. For instance, we can start by considering a square S_t with sidelength $2t$, and the function φ_t having value t at the center, vanishing at the boundary ∂S_t and linear in each of the four subtriangles obtained by a criss-cross splitting of S_t. An elementary computation shows that

$$|\varphi_t|^2_{1,S_t} = 4t^2, \qquad \int_{S_t} \varphi_t \mathrm{d}x\mathrm{d}y = \frac{4t^3}{3}. \tag{2.26}$$

Now we choose b_k in S_t as a multiple of φ_t, in such a way that

$$\int_{S_t} b_k \mathrm{d}x\mathrm{d}y = -\frac{|I_k|}{8}. \tag{2.27}$$

This easily gives $b_k = -\dfrac{3|I_k|\varphi_t}{32t^3}$, and consequently, using (2.26)

$$|b_k|^2_{1,S_t} = 9|I_k|^2/256t^4. \tag{2.28}$$

It is easy to check (see figure 2.2)) that we can always fit inside T_k a little square S_t that does not intersect T_t, provided that $t \leq |I_k|/4\sqrt{2}$. Using the equality, and substituting the corresponding value of t in (2.28)) we get

$$|b_k|^2_{1,S_t} = 36|I_k|^{-2}. \tag{2.29}$$

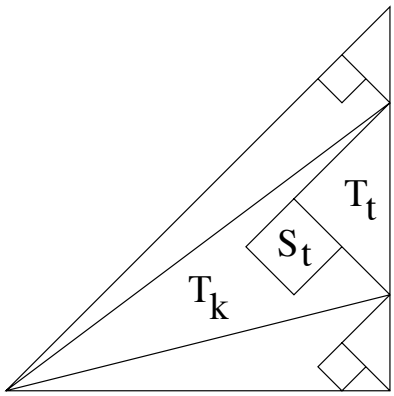

FIG. 2.2.

Finally, with this new choice of b_k, using (2.24) and (2.29), we have

$$\gamma_k^a = |b_k|^2_{1,T_k} = |b_k|^2_{1,T_t} + |b_k|^2_{1,S_t} = 42|I_k|^{-2}. \tag{2.30}$$

In this case the scheme (2.19) becomes

$$\begin{aligned} &a(u_L, v_L) - < u_L, \frac{\partial v_L}{\partial n} > - < v_L, \frac{\partial u_L}{\partial n} > + \textstyle\sum_k 42\, u_L(m_k) v_L(m_k) = \\ &(f, v_L) - < \psi_h, \frac{\partial v_L}{\partial n} > + \textstyle\sum_k 42\, \psi_h(m_k) v_L(m_k). \end{aligned} \tag{2.31}$$

We come back now, briefly, to the Schur complement operator S_h, as described in (2.9). It is easy to see that S_h is the discretization of a pseudo-differential operator S, of order 1, on Σ. More precisely, in this case S is the operator acting in the following way: given a function $\varphi \in H^{1/2}_{00}(\Sigma)$, we first construct the two harmonic functions u^1 and u^2 (in Ω^1 and Ω^2 respectively) having trace equal to φ on Σ and zero elsewhere on $\partial\Omega_i$ $(i = 1, 2)$. The operator S applied to φ is now given on Σ by

$$S\varphi = \frac{\partial u^1}{\partial n_1} + \frac{\partial u^2}{\partial n_2}. \tag{2.32}$$

In order to precondition (2.8) one has to find a cheaply computable operator that could be regarded as an approximation of S^{-1}. Several choices for that are found in the literature. For instance one could solve local Neumann problems in order to get an approximation of the local Steklov-Poincaré operators. Or one can define a sort of $H^{1/2}$ inner product on Φ_h, and invert the associated linear operator. We refer to the survey [10], and to the impressive set of proceedings of the various meetings on Domain Decomposition Methods, whose last volume is [3]. It is clear, however, that in doing that the task is made much easier if the grid on Σ is uniform, as it was the case in our experiments. For instance one could use fast solvers for the local Neumann problems, or find easy expressions for the $H^{1/2}$ inner product. In particular, we used an FFT algorithm for going from a function φ_h to his Fourier (sine) coefficients $\mathbf{c}^\varphi$. Then both the above choices become easy. For instance, the second one ($H^{1/2}$ inner product) corresponds to take, for each frequency n, the product of c_n^φ times n and then transform back. The first one (local Neumann problems) actually came out to

be a minor variant of the first. If L_1 and L_2 are the widths of the two subdomains Ω^1 and Ω^2, respectively, the coefficient c_n^φ has to be multiplied by $n(\tanh(L_1)+\tanh(L_2))$ instead of n.

Both choices, as we shall see in the next section, gave very good results, in particular when the grids in the two subdomains Ω_i were not too coarse compared with the interface grid for ψ. This is very reasonable, as we used, somehow, something close to S to precondition S_h, which is clearly good only for h small enough.

3. Numerical experiments. The above formulation was tested on the academic problem

$$-\Delta u = f \quad \text{in } \Omega, \qquad u = g \quad \text{on } \partial\Omega, \tag{3.1}$$

with $\Omega = [-1,1]\times[0,1]$, $f = 0$, $g = x^2 - y^2$, so that the exact solution of (3.1) is $u(x,y) = x^2 - y^2$. Notice that, with this choice, the use of piecewise linear finite elements on uniform grids for u should produce the exact solution at the nodes. Therefore, the only source of errors is the presence of the interface with non-matching grids. The domain Ω was split into two subdomains with interface at $x = 0$, and in each subdomain a uniform decomposition into triangles was taken (see fig. 3.1).

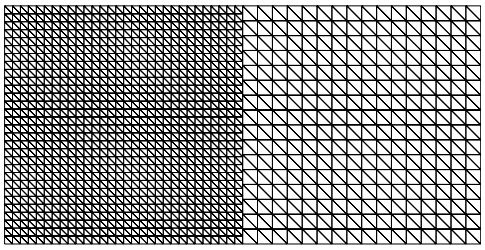

FIG. 3.1. *Example of mesh.*

For each coupling of non-matching grids for the $u-$variable, various meshes at the interface were taken for the $\psi-$variable, in order to see if and how the presence of very small intervals in $\mathscr{T}_\lambda^s$ can influence the performance of the method. Apparently, this fact does not in practice alter the convergence of the scheme. In [8] a crucial hypothesis for deriving error estimates for the $\psi-$variable was that each interval I_ψ must contain at least two regular intervals of $\mathscr{T}_\lambda^s$. The experiments carried out so far showed that this is not necessary in practice.

In figs. 3.2-3.3 we report the behaviour of the error for u, λ, ψ respectively as $\mathscr{T}_\psi$ varies, while the meshes for u are kept fixed: $\mathcal{T}_u^1 = 30\times 30$, $\mathcal{T}_u^2 = 16\times 16$. From these results we see that the best values are reached when the number of nodes of $\mathscr{T}_\psi$ is in between those of $\mathcal{T}_{u\,|\Sigma}^1$ and $\mathcal{T}_{u\,|\Sigma}^2$ (i.e., in between 16 and 30 in our case). When $\mathscr{T}_\psi$ is too coarse we have a natural loss of accuracy. On the other hand, taking an unnecessary fine grid for ψ does not improve the accuracy (it would be unrealistic to expect that), but does not spoil it, and the results are pretty stable. This is particularly true for the most important unknowns, namely, u and ψ.

We also wanted to test the dependence of the quality of the scheme with respect to γ_k^a. For this, we chose different values of γ_k^a of the type $\gamma_k^a = \gamma|I_k|^{-2}$ as in (2.24)

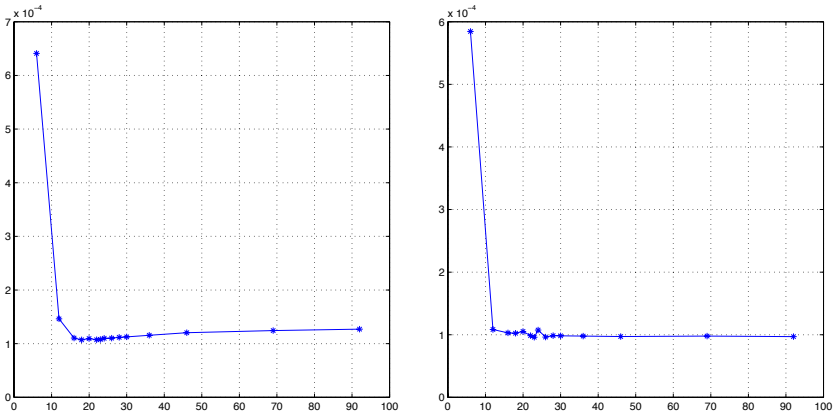

FIG. 3.2. *(a) Error on u (left); (b) Error on u (right).*

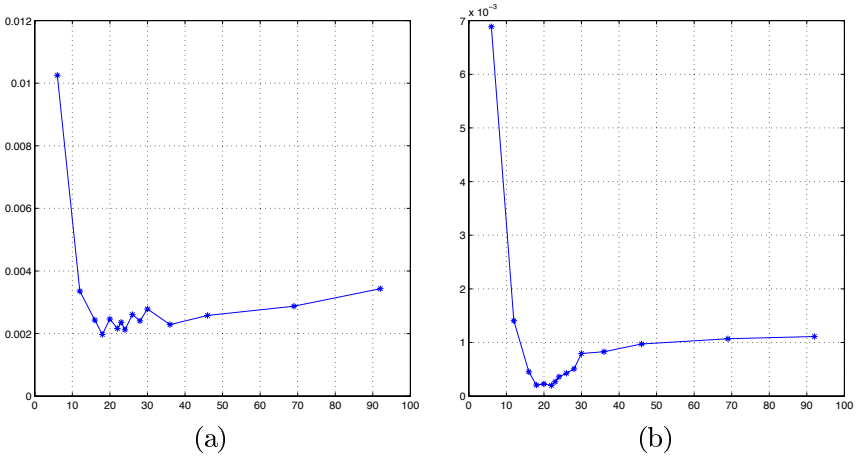

FIG. 3.3. *(a) Error on λ (right); (b) Error on ψ.*

and (2.30), with γ varying from 0.75 up to 360. Fig. 3.4 shows the error on u (on the right) as a function of γ, for the same grids for u as before, and 22 internal nodes for ψ at the interface. We can clearly see that big changes in γ have very little impact on the results.

Another kind of test was meant to check the error estimates proved in [8]. For this, various coupling of meshes in the two subdomains were taken:

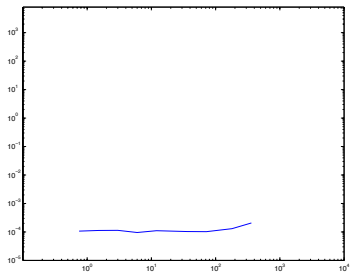

FIG. 3.4. *Dependence of u (right) on γ.*

$$\begin{array}{l} \mathcal{T}_u^1 = [10 \times 10];\ [20 \times 20];\ [30 \times 30];\ [40 \times 40];\ [50 \times 50] \\ \mathcal{T}_u^2 = [8 \times 8];\ [16 \times 16];\ [24 \times 24];\ [32 \times 32];\ [40 \times 40] \end{array} \tag{3.2}$$

According to the suggestions from the previous results, the corresponding $\mathcal{T}_\psi$ was

$$\mathcal{T}_\psi = [9;\ 18\ ;\ 27;\ 36;\ 45]. \tag{3.3}$$

The test was also meant to assess the quality of the preconditioners proposed in the previous section. We solved (2.8) with preconditioned conjugate gradient, stopped when a reduction of 10^{-12} on the initial residual was achieved. Both preconditioners behaved similarly, and the number of iterations to achieve convergence was [5; 7; 8; 8; 8] for $\mathcal{T}_\psi$ as in (3.3). Figs. 3.5-3.6 show the corresponding errors on a log log scale. In each figure the line in the lower left corner represents the theoretical order of convergence. As it can be seen, the slope of the experimental results matches very well that predicted by the theory.

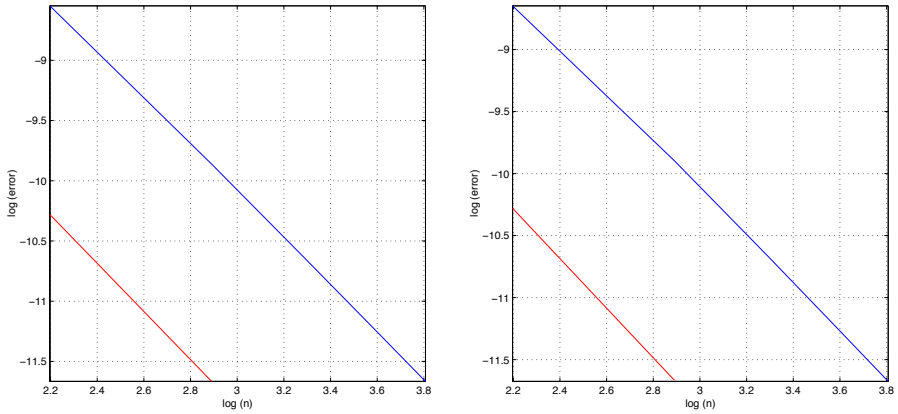

(a) (b)

FIG. 3.5. *(a) Order of convergence for u (left); (b) Order of convergence for u (right).*

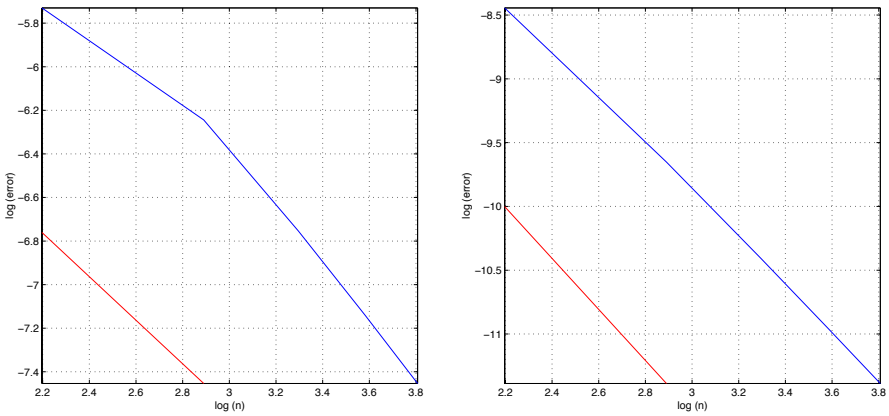

FIG. 3.6. *(a) Order of convergence for λ (right); (b) Order of convergence for ψ.*

REFERENCES

[1] C. BAIOCCHI, F. BREZZI, AND L.P. FRANCA, *Virtual bubbles and Ga.L.S.*, Comp. Meth. in Appl. Mech. and Eng., 105 (1993), pp. 125–141.

[2] P.E. BJØRSTAD AND O.B. WIDLUND, *Iterative methods for the solution of elliptic problems on regions partitioned into substructures*, SIAM J. Numer. Anal., 23 (1986), pp. 1093–1120.

[3] P.E. BJØRSTAD, M.S. ESPEDAL AND D.E. KEYES (EDS.), *Domain Decomposition Methods in Science and Engineering*, Domain Decomposition Press, Bergen, 1998.

[4] J.H. BRAMBLE, J. PASCIAK AND A. SCHATZ, *The construction of preconditioners for elliptic problems by substructuring, IV*, Math. Comput., 53 (1989), pp. 1–24.

[5] F. BREZZI, L.P. FRANCA, L.D. MARINI, AND A. RUSSO, *Stabilization techniques for domain decomposition methods with non-matching grids.* In Domain Decomposition Methods in Science and Engineering, (*9th* International Conference, Bergen, Norway, 1996) P. Bjørstad et al., ed., Domain Decomposition Press, Bergen, 1998, pp. 1–11.

[6] F. BREZZI AND L. D. MARINI, *Macro hybrid elements and domain decomposition methods*, in Optimization et Controle, J. Desideri et al., ed., Toulouse, 1993, CÉPADUÈs-Editions, pp. 89–96.

[7] ———, *A three-field domain decomposition method*, in Domain Decomposition Methods in Science and Engineering, A. Quarteroni et al., ed., Providence, 1994, AMS, Series CONM 157, pp. 27–34.

[8] ———, *Error estimates for the three-field formulation with bubble stabilization.* Math. of Comp., to appear.

[9] A. BUFFA, *Error estimate for a stabilized domain decomposition method with nonmatching grid.* Numer. Math., submitted.

[10] T.F. Chan and T.P. Mathew , *Domain decomposition algorithms*, Acta Numerica 1994, pp. 61–144.

[11] M. DRYJA, *A finite element-capacitance method for elliptic problems on regions partitioned into subregions*, Numer. Math., 44 (1984), pp. 153–168.

[12] R. GLOWINSKI, W.K. KINTON AND M.F. WHEELER, *Acceleration of domain decomposition algorithms for mixed finite elements by multilevel methods* , in Third Int. Symp. on Domain decomposition methods for partial differential equations, T. Chan et al., ed., SIAM (Philadelphia), 1990.

[13] G. GOLUB AND D. MAYERS, *The use of preconditioning over irregular regions*, in Computing Methods in Applied Sciences and Engineering, VI, R. Glowinski and J.L. Lions, eds., North Holland, 1984, pp. 3–14.

[14] YU. A. KUZNETSOV AND M.F. WHEELER, *Optimal order substructuring preconditioners for mixed finite element methods on nonmatching grids*, East-West Journal of Numerical Mathematics, 3 (1995), pp. 127–144.

[15] B.F. SMITH AND O.B. WIDLUND, *A domain decomposition algorithm using a hierarchical basis*, SIAM J. Sci. Comput., 11 (1990), pp. 1212–1220.

[16] C.H. Tong, T.F. Chan and C.C.J. Kuo, *A domain decomposition preconditioner based on a change to a multilevel nodal basis*, SIAM J. Sci. Comput., 12 (1991), pp. 1486–1495.
[17] J. Xu, *Theory of multilevel methods*, PhD thesis, Cornell University, 1989.